# A comparative study of olefin or acetylene insertion into Ru–H or Os–H of MHCl(CO)(phosphine)$_2$

**Alexei V. Marchenko,[a] Hélène Gérard,[b] Odile Eisenstein*[b] and Kenneth G. Caulton*[a]**

[a] *Department of Chemistry, Indiana University, Bloomington, IN 47405-7102, USA. E-mail: caulton@indiana.edu*

[b] *Laboratoire de Structure et Dynamique des Systèmes Moléculaire et Solides (CNRS UMR 5636), Université de Montpellier 2, 34095 Montpellier cedex 05, France. E-mail: eisenst@lsd.univ-montp2.fr*

***Received (in New Haven, CT, USA) 26th March 2001, Accepted 10th July 2001***
***First published as an Advance Article on the web 19th October 2001***

The adduct OsHCl($C_2D_4$)(CO)$L_2$ (L = P$^i$Pr$_3$) shows only very slow H/D exchange at 25 °C, but this is easily detectable at 65 °C; no ethyl species is formed in detectable concentration. RuHCl(CO)$L_2$ shows no detectable $C_2D_4$ adduct, but Ru–H/C–D exchange at 60 °C is actually faster than for Os. DFT (B3PW91) calculations have been carried out to analyze the relative energies of the isomeric forms that would result from the addition of an alkene or an alkyne to MH(Cl)(CO)($PH_3$)$_2$ (M = Os, Ru). Thus, 18-electron alkyne adducts are compared to the 18-electron vinylidene isomer and to the 16-electron vinyl complex. Similarly, the 18-electron alkene adduct is compared to the 18-electron carbene isomer and to the 16-electron ethyl complex. Two factors are found to control the products formed: (i) the Os complex favors unsaturated π-bonded ligands and an 18-electron count while Ru favors saturated ligands and an unsaturated metal center; (ii) the weaker π bond in the alkyne than in the alkene makes insertion or isomerization of an alkyne thermodynamically more favored than that of an alkene. This results in ethyl complexes being less favored than vinyl complexes in similar experimental conditions. For RuHCl(CO)$L'_2$, where L′ is P$^i$Pr$_2$[3,5-(CF$_3$)$_2$C$_6$H$_3$], 1 atm ethylene gives a detectable, colorless ethylene adduct, then also a detectable ethyl complex, all in facile equilibrium.

The five-coordinate, 16-electron square-pyramidal molecules MHCl(CO)$L_2$ (L = P$R_3$; M = Ru and Os) provide a rich variety of reactions with unsaturated hydrocarbons.[1–5] For L = P$^i$Pr$_3$, the osmium complexes form 1 : 1 adducts (**1**) with olefins [$H_2C$=CHR with R = H, $CO_2$Me, CN, C(O)Me] and, ". . . probably owing to the *trans* position of these (H and olefin) ligands",[3] there is no insertion of the olefin into the Os–H bond to form an alkyl. However, RuHCl(CO)(P$^i$Pr$_3$)$_2$ and ethylene are completely unreactive.[3] In contrast, both Ru and Os complexes with L = P$^i$Pr$_3$[3] and P$^t$Bu$_2$Me[4] add M–H across the RC≡CH bond for R = H, Me and Ph within 30 min at 25 °C, to give unsaturated vinyl complexes (**2**).

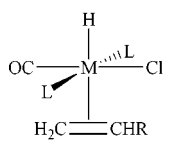


**1**

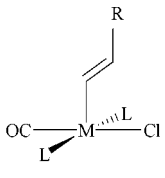


**2**

Regarding the mechanism, it was stated that: "Addition of the alkyne to the metal first occurs, followed by rapid migration of the hydride from the metal to the carbon atom."[5a] The lack of M–H addition to C=C but rapid addition to C≡C is not only paradoxical, but it emphasizes how much is unknown about these reactions, in which the LUMO (**3**) would suggest formation of an adduct

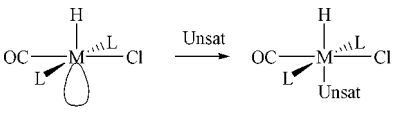


(1)

**3**

[eqn. (1)] with stereochemistry unsuitable (*i.e.*, H and the reducible ligand mutually *trans*) for H transfer to carbon. We report here an experimental and computational study of the addition of the M–H of MH(CO)Cl$L_2$ across the C=C bond of ethylene, including the influence, on the addition thermodynamics, of a less electron-donating L and of changing from Ru to Os.

## Results

### Isotope exchange evidence for an osmium ethyl

The reaction of OsHCl(CO)$L_2$ (L = P$^i$Pr$_3$) with ethylene stands as an interesting example. The $^1$H NMR spectrum of red OsHCl(CO)$L_2$ in $C_7D_8$ under 250 mm ethylene at 25 °C shows complete formation of a colorless 1 : 1 adduct[6] with spectral features distinct from that of the five-coordinate reagent complex. The color change from red to colorless also speaks for essentially complete (>95%) adduct formation. The $^{31}$P{$^1$H} NMR signal is a sharp singlet at 18.1 ppm; no OsHCl(CO)$L_2$ is seen by $^{31}$P NMR. The Os–*H* chemical shift, −4.7 ppm (triplet) is sufficiently downfield from the value (−32.5 ppm) in OsHCl(CO)$L_2$ to indicate that a ligand is *trans* to hydride. A somewhat broad ($\Delta\nu_{1/2}$ = 17.5 Hz) resonance is seen for four hydrogens of coordinated $C_2H_4$, at 2.9 ppm, compared to a broader resonance at 5.3 ppm for free ethylene. At −20 °C, the hydride signal and the line due to free $C_2H_4$ are both detectably sharper, due to slower site exchange by the process in eqn. (2). This indicates that $k_1 \cdot$[OsHCl(CO)$L_2$] is large enough to shorten the lifetime of free $C_2H_4$; that is, OsHCl(CO)$L_2$ is present at a kinetically

 DOI: 10.1039/b103113a

significant (but not directly observable) concentration at +25 °C.

$$OsHCl(CO)L_2 + C_2H_4 \underset{k_{-1}}{\overset{k_1}{\rightleftharpoons}} \text{(H, OC, L, Cl, L, } C_2H_4\text{ on Os)} \qquad (2)$$

Even after 5 h at 25 °C in this experiment, there is no appearance of any new product, such as $Os(C_2H_5)Cl(CO)L_2$. To test for a thermally accessible, but essentially unpopulated (<0.05 mol fraction) ethyl complex, $OsDCl(CO)L_2$ was reacted with $C_2H_4$. The $^1H$ and $^2H$ NMR spectra of the resulting $OsDCl(C_2H_4)(CO)L_2$ were followed over time in $C_6H_6$. After 5 h at 20 °C, the OsD signal is still strong but the $^2H$ NMR shows a weak signal for coordinated deuterated ethylene (2.9 ppm). By $^1H$ NMR, free and coordinated ethylene are evident and OsH is undetectable. After this solution is heated at 65 °C for 23 h, the $^2H$ NMR spectrum at 25 °C shows reduced D on osmium and increased D on coordinated ethylene. The $^1H$ NMR spectrum shows reduced signal intensity for both free and coordinated ethylene, and also the growth of a signal for $OsHCl(ethylene)(CO)L_2$ at −4.6 ppm.[7] Taken together, all of these observations indicate that D on osmium is incorporated into ethylene (including dissolved and vapor phase ethylene). Two possible routes for this H/D exchange will be discussed in the computational studies. The H/D exchange is slow at 25 °C. While heating to 65 °C accelerates the reaction, the fact that the solution is red in color at *this* temperature shows that the equilibrium in eqn. (2) shifts significantly away from the adduct ($\Delta S$ for adduct formation is negative). It is thus suggested that the product of addition of ethylene to site **a** in **4** does not mediate H/D exchange. Finally, the deuterium distribution, over 50% on Os after 23 h at 65 °C, is still far from the equilibrium situation, so ethyl formation is slow under these reaction conditions.

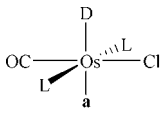


**4**

It was confirmed that the red color of $OsHCl(C_2H_4)(CO)L_2$ under $C_2H_4$ at +65 °C is *not* due to formation of an $Os–CH_2CH_3$ species by observing the $^1H$ and $^{31}P$ NMR spectra of $OsHCl(C_2H_4)(CO)L_2$ under 1 atm $C_2H_4$ at elevated temperatures. While the $^{31}P\{^1H\}$ NMR spectrum only broadens with an unaltered chemical shift between +16 and +70 °C in $C_6D_6$, the $^1H$ NMR is more informative. The sharp $^1H$ NMR signals for free and coordinated ethylene and for OsH (triplet) all broaden progressively at their (unaltered) chemical shift values. By 70 °C, the OsH resonance is too broad to show triplet structure, and the "free $C_2H_4$" signal at *ca.* 5.3 ppm has a full-width at half height of 364 Hz. In summary, there is no evidence for any process other than the on/off equilibrium of ethylene onto $OsHCl(CO)L_2$. In particular, there is no evidence for population of any $Os–CH_2CH_3$ species at the 5% mol fraction detection limit.

This isotope exchange was also monitored from the opposite direction: $OsHCl(CO)L_2$ was held at 60 °C in $C_6H_6$ for 27 h under 500 mm $C_2D_4$. The $^1H$ NMR at 20 °C after this thermal treatment shows that the $OsHCl(ethylene)(CO)L_2$ contains only trace amounts of proton in the coordinated and free ethylene and only trace residual protons on Os (it is mostly Os–D because of the high molar ratio of $C_2D_4$ : Os in the NMR tube). The $^2H$ NMR of this same sample shows (in addition to dissolved ethylene-$d_n$) a lot of coordinated ethylene-$d_n$ and a strong Os–D signal. There was no significant deuteration of any P–$^i$Pr site.

**Comparison to ruthenium.** Does the weak (*i.e.*, undetectable under 1 atm $C_2H_4$ at 25 °C) binding of ethylene to $RuHCl(CO)L_2$ already mentioned in the Introduction prevent addition of Ru–H across C=C? To answer this, the analogous H/D exchange experiment was carried out with $RuHCl(CO)L_2$ and 700 mm $C_2D_4$. Here, since no detectable ethylene adduct is present at the 20 °C NMR measurement temperature, one observes only Ru(hydride)$Cl(CO)L_2$. The $^1H$ NMR spectrum after 27 h at 60 °C shows negligible (S/N ≈ 2) hydride intensity. The $^2H$ NMR spectrum of the same sample shows a strong Ru–D peak (and free ethylene-$d_n$), but also deuteration of the $^i$Pr methyls to an average population of 0.8 sites per Ru–D. This pendant alkyl deuteration, although slow, is significantly faster than in the osmium analog. The H/D scrambling is thus consistent with olefin insertion into the Ru–H bond, but without giving any detectable quantity of the ethyl complex.

## DFT comparison of the ethylene/ethyl/carbene and alkyne/vinyl/vinylidene isomers for Ru and Os

A computational study has been carried out to analyze the energies of the three isomers that could be expected from the reaction of an alkene (modeled by $C_2H_4$) with $MHCl(CO)(PH_3)_2$ (M = Ru and Os). Comparison with the case of an alkyne (modeled by $C_2H_2$) enhances our understanding of some factors controlling the energy pattern for the insertion reaction. Although the experimental results presented in this work focus essentially on the products of insertion of ethylene into the M–H bond, comparing these computational results to those for other transformations than can occur in the coordination sphere of the metal center (ethylene into carbene and alkyne into vinylidene) gives a more global understanding of the potential to transform these two ligands. Thus, for the reaction with alkene, the 18-electron ethylene adduct will be compared to the 18-electron CHMe isomer and to the 16-electron ethyl complex. The energy pattern thus obtained is contrasted to that for 18-electron alkyne, 18-electron vinylidene and 16-electron vinyl complexes, which have been already partially discussed.[8] The resulting DFT (B3PW91) energy patterns, shown in ($C_2H_4$) and ($C_2H_2$), show trends that agree with the experimental observations.

**The ethylene/ethyl transformation.** The alkene is more strongly bonded to $OsHCl(CO)(PH_3)_2$ (25.7 kcal mol$^{-1}$) than to its Ru analog (17.0 kcal mol$^{-1}$) (step a, Fig. 1), as expected from the higher back-donating ability of Os. The small calculated value of the binding energy for Ru as well as entropy [free energy of binding ethylene to $RuHCl(CO)(PH_3)_2$ at 298 K is 2.7 kcal mol$^{-1}$], which favor alkene loss, account for the lack of observation of the $RuHCl(alkene)(CO)(P^iPr_3)_2$ adduct, as reported in this work. The energy of reaction for the formation of the alkyl complex from *separated* reactants (step e) is remarkably independent of the nature of the metal (difference of less than 1 kcal mol$^{-1}$ between Os and Ru) and is significantly exothermic. The geometry of the ethyl complex is that of $MHCl(CO)(PH_3)_2$ with a non-agostic ethyl in place of hydride. The independence with respect to the metal suggests that the σ M–H and the M–C alkyl binding energies vary similarly with the metal, which is the case for many systems.[9] Step b of Fig. 1 is the transformation of the ethylene complex to the alkyl isomer. This step, which can be considered, for the sake of the thermodynamic analysis, as being composed of ethylene decoordination (reverse of step a), followed by insertion of the ethylene in the M–H bond (step e), has an energy pattern determined by that of step a. Therefore,

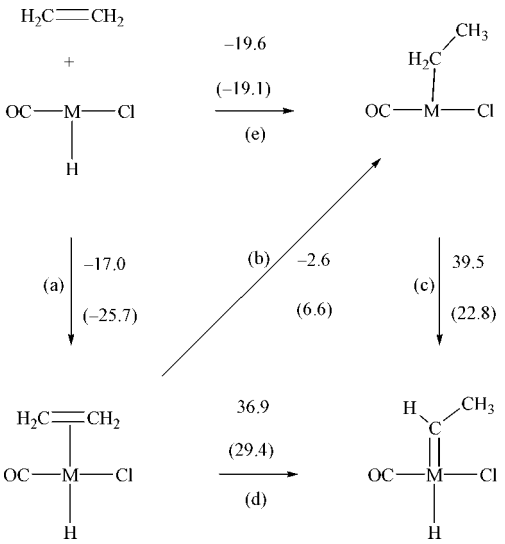


**Fig. 1** Thermodynamic cycle (reaction energies in kcal $mol^{-1}$) for $C_2H_4$ reacting with $MHCl(CO)(PH_3)_2$ (M = Ru, Os). Values for Os are in parentheses. Out-of-plane $PH_3$ ligands are omitted, for clarity.

step b is essentially thermoneutral for Ru and slightly endothermic for Os, as expected from the loss of the energetically more important π back-donation for Os.

The isodesmic reaction [eqn. (3)] summarizes the thermodynamic preference of Ru and Os for the 16-electron ethyl and the 18-electron ethylene complexes.

$$RuHCl(C_2H_4)(CO)(PH_3)_2 + Os(C_2H_5)Cl(CO)(PH_3)_2 \rightarrow OsHCl(C_2H_4)(CO)(PH_3)_2 + Ru(C_2H_5)Cl(CO)(PH_3)_2 \quad (3)$$

This $\Delta E$ value of $-9.2$ kcal $mol^{-1}$ is large enough so as not to be reversed by changes in the level of calculations or the nature of the substituent on the olefin and the nature of the phosphine. Thus, whereas the transformation of an olefin into an ethyl complex may be feasible or not, depending on the nature of ligands and substituents (*i.e.*, $\Delta E$ of step b of Fig. 1 is small), it is certain that there is a significantly greater probability of observing an alkyl complex for Ru than for Os. Even though the ethyl complex with $P^iPr_3$ was not accumulated in sufficient quantity to allow detection with either Ru or Os, the faster H/D scrambling with Ru than Os is consistent with the ethyl complex being energetically more accessible with Ru.

What is also clear from Fig. 1 is that, for osmium, the $\eta^2$-ethylene complex has become the global minimum, so that the ethyl isomer will not be detectably populated. For ruthenium, the ethyl isomer is calculated to be detectable because the $\eta^2$-ethylene species is not as deep a minimum. Fig. 1 also shows that the formation of the ethyl complex from separated reactants is essentially metal-independent and therefore also likely insensitive to ligand *electronic* effects. Thus, the phosphine electronic effect will influence primarily the relative energy of the $\eta^2$-olefin adduct. Therefore, the equilibrium molar fraction of the ethyl can be estimated by evaluating the back-donor capacity of the metal ligand set. Steric effects must then be evaluated independently.

**The ethylene/carbene transformation.** The isomerization of the ethylene complex to the CHMe complex (step d of Fig. 1) is highly endothermic, although it is less disfavored for Os (endothermic by 29.4 kcal $mol^{-1}$) than for Ru (endothermic by 36.9 kcal $mol^{-1}$). This indicates that the CHMe carbene requires more stabilization *via* back-donation than the alkene, that is, CHMe is a stronger π acid than $\eta^2$-ethylene in this environment. Step c illustrates the greater stability of the unsaturated 16-electron alkyl complex over its saturated 18-electron CHMe isomer (the ethyl complex is more than 20 kcal $mol^{-1}$ more stable than the carbene).[10] The insertion of the carbene into the Os–H bond predicted by step c has been reported earlier[11,12] and the *meta*stability of carbene complexes using the same metal fragment is established to be of kinetic origin.[12] The greater thermodynamic preference for an alkyl structure over an isomer with a π-bonded ligand for Ru than for Os reiterates the results obtained above for ethylene. This trend has been noted in a number of systems with various types of ligands.[13] It derives from the larger metal–ligand binding energies in the case of Os, which results in the qualitative rule: Ru favors isomers that maximize bonds within the organic ligands (*i.e.*, alkyl), whereas Os has a relatively greater preference for more ligand–metal bonds (*i.e.*, hydrido-carbene). The analysis of the thermodynamic cycles of Fig. 1 shows that the difference lies in the strong bonding of the π acid (and thus unsaturated) organic ligand to the Os center. This favors the unsaturated organic ligand bound at the electron-rich Os center *vs.* the saturated organic ligand bound to the less π-basic Ru center.

**Comparison with the alkyne/vinyl/vinylidene isomers for Ru and Os.** Going to the analogous studies for the alkyne (Fig. 2) allows for a better understanding of the role of the ligand itself. Why is insertion into M–H more often observed for alkyne than for alkene? The influence of the metal on each individual step uniformly follows the trends noted above for ethylene. This discussion will thus focus on comparing the acetylene and ethylene for each individual step in Fig. 1 and 2. Step a shows that ethylene binds more strongly to the metal fragment than acetylene; this order is also true for $\Delta G$. Numerous discussions have been devoted to this problem.[14] Acetylene behaves like a two-electron donor when bonded to a 16-electron square-pyramidal fragment since there is no empty metal d orbital to receive electrons from the acetylene π bond perpendicular to the C–M–C plane. This π orbital leads, in fact, to four-electron repulsion with the symmetry-adapted occupied d orbital (**5**). As in the case of ethylene (Fig. 1), the energy of reaction for insertion of free acetylene into the M–H bond (step e, Fig. 2) is remarkably independent of the metal. This is indicative of little or no metal π donation into the vinyl ligand. The formation of the vinyl complex from free acetylene and a given metal fragment is around 20 kcal $mol^{-1}$ more exothermic than for the formation of the ethyl complex from free ethylene (*i.e.*, step e). This is a dramatic contrast and the preference is consistent with experiment. The much larger energy of the π bond in free ethylene in comparison to one of the π bonds in acetylene is the cause of this result.[15] Since acetylene binds less strongly to the metal (step a) and since there is a larger gain in energy associated with the insertion into the M–H bond (step e), the transformation of the 18-electron $MHCl(C_2H_2)(CO)(PH_3)_2$ into the 16-electron vinyl complex is thermodynamically very favorable for both Ru and Os. This result agrees very well with the observations that the vinyl complex is the thermodynamic product for the reaction of any alkyne with $MHCl(CO)L_2$ for both Ru and Os.[8]

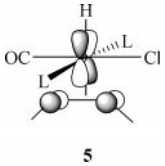


**5**

The transformation of the acetylene complex into the vinylidene complex (step d of Fig. 2) has been the topic of a number of theoretical analyses.[16,17a–f] The thermodynamics of the reaction is significantly dependent on the metal

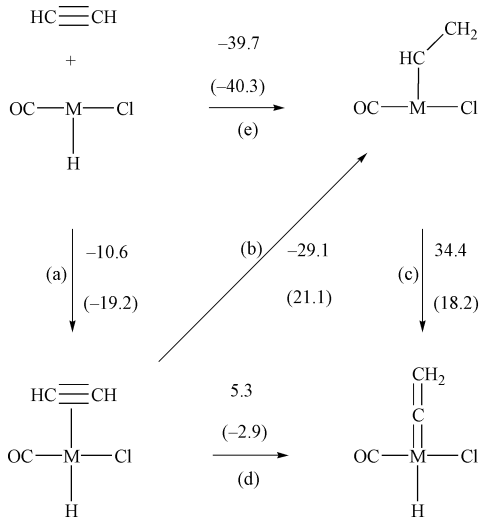


**Fig. 2** Thermodynamic cycle (reaction energies in kcal $mol^{-1}$) for $C_2H_2$ reacting with $MHCl(CO)(PH_3)_2$ (M = Ru, Os). Values for Os are in parentheses. Out-of-plane $PH_3$ ligands are omitted, for clarity.

fragment. For the transformation of the (*carbonyl-free*) 16-electron $RuHCl(C_2H_2)(PH_3)_2$ into the 16-electron $RuHCl(CCH_2)(PH_3)_2$, the reaction is exothermic (11.9 kcal $mol^{-1}$ using the current level of calculations).[16] In the presence of an additional CO ligand, the corresponding transformation (step d of Fig. 2) becomes slightly endothermic (5.3 kcal $mol^{-1}$). This illustrates how a π acid spectator ligand disfavors the isomerization of the alkyne into a more π acidic isomer (vinylidene). In agreement with this argument, increasing the electron donating ability of the metal (Ru replaced by Os) makes step d more exothermic (−2.9 kcal $mol^{-1}$ for Os *vs.* +5.3 kcal $mol^{-1}$ for Ru). Experimental observations[8] support these numerical results. The greater thermodynamic preference for isomerizing the coordinated alkyne into coordinated vinylidene in comparison to isomerizing the coordinated olefin into coordinated carbene has also been discussed for the $RuHClL_2$ fragment.[16] The determining factor has been shown to be the lower energy for isomerizing $C_2H_2$ into $C{=}CH_2$ in comparison to $C_2H_4$ into $CH(CH_3)$. The results for the $MHCl(CO)L_2$ fragments are analogous.

In summary, the factors that appear to determine the relative energies of these isomeric forms are: (i) the stronger energy of the π bond of free olefin in comparison to that of one π bond in free alkyne, (ii) the greater capability for Os than Ru to backbond into an organic ligand, and (iii) the fact that M–H and M–C σ bond energies vary similarly, at least for metals belonging to the same column of the periodic table. It is also important to keep in mind that these energy patterns describe exclusively thermodynamic preferences and that kinetic information is required to understand how rapidly these species are interconverted.

We also considered a second exchange mechanism, that of oxidative addition of an ethylene C–H bond to the metal to give a M("2H")Cl($CH{=}CH_2$)$(PH_3)_2$ species. In the present case of Os, a vinyl complex with the two H centers as an $H_2$ ligand[17g] has been located as another minimum 37 kcal $mol^{-1}$ above the ethyl complex. Although no calculations of the reaction path have been carried out, this result suggests that the H/D exchange that has been observed in the reaction of $OsDCl(CO)L_2$ is best explained as occurring *via* an ethyl complex that does not accumulate enough to be observed rather than by vinyl C–H oxidative addition.

### An observable ethyl species in equilibrium with free ethylene

Since the insertion of ethylene into the Ru–H bond (step b of Fig. 1) was calculated to be thermoneutral for $PH_3$ as the model phosphine, a change in the phosphine ligand may allow the observation of the products of ethylene insertion. We thus considered the Ru complex[18] with an electron-withdrawing phosphine substituent: 3,5-$(CF_3)_2C_6H_3 \equiv Ar^F$. When $RuHCl(CO)(P^iPr_2Ar^F)_2$ is subjected to a *ca.* 20-fold excess of ethylene, the solution first becomes colorless, *then* rosy within 10 min of mixing at +20 °C. $^1H$ NMR shows a broad hydride peak at −10.93 ppm, as well as a new broad peak at 2.77 ppm assigned to coordinated ethylene. Free ethylene is also seen. Along with the $^{31}P\{^1H\}$ NMR chemical shift at 54.4 ppm [74% of product intensity and due to coalesced $RuHCl(CO)(P^iPr_2Ar^F)_2$ and ethylene adduct], this is indicative of an equilibrium involving coordination of ethylene *trans* to the hydride. Upon cooling to +7 °C, the broad hydride chemical shift moves to −8.36 ppm and the $^{31}P\{^1H\}$ NMR chemical shift moves to 52.9 ppm, due to the increase in the molar fraction of the adduct in the equilibrium mixture, but still in a rapid exchange (*i.e.*, coalesced) regime. Already at 20 °C, a second product is also formed; $^{31}P\{^1H\}$ NMR also shows a signal at 40.8 ppm (26%), in a region of chemical shifts typical of unsaturated complexes: Ru(hydrocarbyl)Cl(CO)$(P^iPr_2Ar^F)_2$ (red-colored). The rosy color of the solution also suggests the presence of an unsaturated complex, different from the starting material. It is thus reasonable to explain these observations by the presence of the unsaturated ethyl complex $Ru(CH_2CH_3)Cl(CO)$-$(P^iPr_2Ar^F)_2$ in the mixture, which can result from insertion of the ethylene into the Ru–H bond. When ethylene in this reaction mixture is removed by four cycles of freeze–pump–thawing, the only species remaining is the five-coordinate $RuHCl(CO)L_2$, thus demonstrating the reversibility of both ethylene addition and insertion.

The variable-temperature $^{31}P\{^1H\}$ and $^1H$ NMR spectra of $RuHCl(CO)(P^iPr_2Ar^F)_2$ were studied in $d_8$-toluene under *ca.* 2 atm ethylene, and give evidence for the presence of an equilibrium between the unsaturated hydride complex and an $\eta^2$-ethylene adduct. The equilibrium between these two is rapid at 20 °C, and the averaged $^{31}P$ and Ru–H chemical shifts give a $RuHCl(CO)(P^iPr_2Ar^F)_2$ population of 47 and 43%, respectively, of the ethylene adduct. Also present at 41.4 ppm is a $^{31}P\{^1H\}$ NMR signal, with an intensity of 32% of that for the exchange-averaged signal, due to the ethyl complex $Ru(C_2H_5)Cl(CO)(P^iPr_2Ar^F)_2$; this peak remains unchanged in chemical shift and linewidth at −20, −40, −60 and −70 °C. The spectra of the exchange-averaged RuP and Ru–H signals undergo dynamic behavior typical of decoalescence in a dissociative equilibrium [eqn. (4)]. The hydride signal moves from −13.8 to −6.4 (−20 °C),

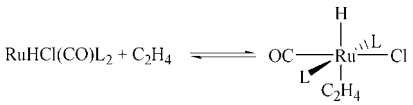

(4)

−5.4 (−40 °C), −4.99 (−60 °C) and −4.90 ppm (−70 °C). The last of these is a well-resolved triplet, while it is already too broad to resolve this P–Os–H coupling at −60 °C. Over this same range of temperatures, the $^{31}P\{^1H\}$ signal moves from 55.5 ppm at +20 °C, to 51.3 (−20 °C), 50.4 (−40 °C), 49.6 (−60 °C) and *ca.* 49.4 ppm (−70 °C). The last two spectra show an increasingly (*vs.* the −40 °C spectrum) broad resonance for what is >95% formed $\eta^2$-ethylene adduct. At −60 and −70 °C, the Ru($\eta^2$-ethylene) : Ru($C_2H_5$) molar ratio is 2 : 1 (integration of the $^{31}P$ NMR intensities). At −60 °C, there are five P–C–H multiplets resolved, which is more than the four expected for two different molecules being present; together with the broadening of the $^{31}P$ signal of the ethylene adduct, this is best explained by hindered rotation[19] about Ru–P and P–C bonds in the six-coordinate (crowded) species. At −60 °C, the $^1H$ NMR resonance of coordinated ethylene (2.58 ppm) broadens. In summary, $RuHCl(CO)(P^iPr_2Ar^F)_2$

and its ethylene adduct are in more rapid equilibrium than are either of these molecules with $Ru(C_2H_5)Cl(CO)(P^iPr_2Ar^F)_2$.

A valuable supplement to this complex picture is provided by the $^2H$ NMR spectrum of $RuHCl(CO)(P^iPr_2Ar^F)_2$ under 10 equiv. of $C_2D_4$. After 10 min at 20 °C, this spectrum shows a signal due to deuterated $\eta^2$-ethylene, but also an Ru–D signal and *one* signal due to the Ru–ethyl–$d_n$ ligand, at 0.68 ppm. This chemical shift is masked by the $^i$Pr signals in the all-protio compound. The $^{31}P\{^1H\}$ NMR spectrum confirms the presence of signals attributed above to the $\eta^2$-ethylene and Ru ethyl complexes. At −20 °C, the $^2H$ NMR signal due to the ethyl-$d_n$ ligand is resolved into two signals separated by 0.1 ppm. The structure of both products of the reaction of $RuHCl(CO)(P^iPr_2Ar^F)_2$ with ethylene is confirmed by the $^{13}C\{^1H\}$ NMR spectral data obtained using $^{13}C$-enriched ethylene as the reagent. $^{13}C\{^1H\}$ NMR of the reaction mixture in $C_6D_6$ shows two new peaks at 10.9 (d, $J_{CC} = 36.6$) and 20.9 ppm (d, $J_{CC} = 36.6$ Hz), which correspond to the $CH_2$ and $CH_3$ carbons of the ethyl complex. Also, there is a broad signal at 40.9 ppm due to the coordinated ethylene of the $\eta^2$-adduct. This NMR data is in good agreement with the previously reported spectral features of a $PCy_3$-containing ruthenium ethyl complex.[20]

The observed reactivity of $RuHCl(CO)(P^iPr_2Ar^F)_2$ towards ethylene is quite remarkable. It shows that a Ru(ethyl) species is energetically achievable simply by modification of the phosphine substituent. The greater stability of the ethylene adduct originates most probably from the diminished steric hindrance of the aryl phosphine. Electronic effects are most likely in the opposite direction since a more electron-poor metal should bind the ethylene less strongly (*cf.* Os *vs.* Ru). Our calculations also show that the energy for inserting *free* olefin into the M–H bond is almost independent of the electronic properties of the metal. Probably the diminished bulk of the aryl phosphine also allows for a greater accumulation of the ethyl complex. The dominant effect of the $^i$Pr → $C_6H_3(CF_3)_2$ change is to make the phosphine smaller. This favors ethylene binding to $RuHCl(CO)L_2$ (*e.g.*, step a, Fig. 1), relative to the separated particles. Detectably populating the ethyl isomer requires avoiding excessive stability of the ethylene adduct, that is, only modest back-donation. A less electron-rich Ru thus favors the ethyl species over the $\eta^2$-$C_2H_4$ species. In summary, $P^iPr_2Ar^F$ contributes to our observation of ethyl and $\eta^2$-ethylene species, probably mostly for steric reasons.

The observed behavior of $RuHCl(CO)(P^iPr_3)_2$ contrasts dramatically with the recent report[20] that a solution containing 50 : 1 ethylene : $RuHCl(CO)(PCy_3)_2$ (Cy = cyclohexyl) forms an adduct essentially completely at −80 °C (although it binds negligibly at +40 °C because $\Delta H^\circ$ is only −12 kcal mol$^{-1}$ but $\Delta S^\circ$ is −45 cal K$^{-1}$ mol$^{-1}$). Moreover, under these same conditions, equilibrium conversion to $Ru(C_2H_5)Cl(CO)(PCy_3)_2$ was also observed, with the $RuHCl(CO)L_2$ to RuEt molar ratio being 1 : 1.7.

## Discussion

The results presented here highlight the difference between the behavior of alkyne and olefin towards insertion into our M–H bonds. Several reasons for the difference have been discussed based on the numerical results of Fig. 1 and 2. While the role of the metal should not be neglected, a key role is played by the organic substrates themselves. The difference in behavior for reaction with an M–H bond parallels the difference in energy of hydrogen transfer among the hydrocarbons, as illustrated by the isodesmic reaction [eqn. (5)], which is endothermic by 11.5 kcal mol$^{-1}$ from experimental and theoretical studies.[21]

$$2\,C_2H_4 \rightarrow C_2H_2 + C_2H_6 \qquad (5)$$

This study shows the experimental reality of insertion of ethylene into the Ru–H bond of $RuHCl(CO)(P^iPr_2Ar^F)_2$, analogous to that recently reported for the $PCy_3$ analog of the ethyl species, as well as a parallel computational study that gives a complete overview of this and competing reactions, and the reason for its low extent of formation. The calculations also permit a simple *understanding* of why the equilibrium degree of formation of ethyl is higher for Ru than for Os. What remains obscure are the phosphine substituent effects: why does replacement of all $^i$Pr of $P^iPr_3$ by cyclohexyl improve the $\Delta G$ of formation of ethyl relative to its closest competitor, the $\eta^2$-$C_2H_4$ isomer? Clearly, bulky phosphines are predicted to favor ethyl over $\eta^2$-$C_2H_4$, but too much bulk can disfavor ethyl relative to Ru–H and free ethylene.

The system under study has an interesting *mechanistic* feature: the "least motion" site for olefin binding is *trans* to hydride, thus frustrating ethyl formation *from this species* [given the generally high barrier for (intramolecular) fluxionality of six-coordinate monohydrides]. However, once formed, the ethyl is thereby somewhat "protected" against the facile β-H migration generally attributed to unsaturated ethyl complexes due to the necessity [eqn. (6)] to

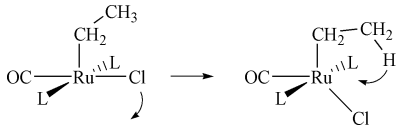

(6)

migrate Cl to create a sterically accessible LUMO. This is perhaps why we observe a slower rate of equilibration of Ru ethyl complex with its precursor.

## Experimental

### General considerations

All reactions and manipulations were conducted using standard Schlenk and glovebox techniques under pre-purified argon. Ethylene and ethylene-$d_4$ were used as received from the manufacturers (Air Products and Cambridge Isotope Laboratories). Solvents were dried and distilled under argon, and stored in air-tight solvent bulbs with Teflon closures. All NMR solvents were dried, vacuum-transferred, and stored in a glovebox. $^1H$, $^2H$, $^{31}P$, and $^{19}F$ spectra were recorded on Varian Gemini 300, Varian Inova 400, and Varian Inova 500 instruments. Chemical shifts are referenced to residual solvent ($^1H$, $^2H$), external $H_3PO_4$ ($^{31}P$), or external $CF_3CO_2H$ ($^{19}F$). $OsHCl(CO)(P^iPr_3)_2$,[1] $RuHCl(CO)(P^iPr_3)_2$, $OsDCl(CO)(P^iPr_3)_2$,[3] and $RuHCl(CO)(P^iPr_2[3,5\text{-}(CF_3)_2C_6H_3])_2$[18] were prepared according to known procedures.

### General technique for conducting reactions of the metal complexes with $C_2H_4$ and $C_2D_4$

NMR tubes were charged with $OsHCl(CO)(P^iPr_3)_2$ or $OsDCl(CO)(P^iPr_3)_2$ (15 mg, 0.026 mmol) or $RuHCl(CO)(P^iPr_3)_2$ (15 mg, 0.031 mmol) or $RuHCl(CO)(P^iPr_2Ar^F)_2$ (15 mg, 0.020 mmol) and benzene-$d_6$ or toluene-$d_8$ (0.5 mL). These solutions were degassed by three freeze–pump–thaw cycles, then the reaction tubes were cooled to −196 °C and $C_2H_4$ or $C_2D_4$ was added at the stated pressure using a vacuum line.

**Reaction of $OsHCl(CO)(P^iPr_3)_2$ with $C_2H_4$.** An orange solution of $OsHCl(CO)(P^iPr_3)_2$ in $C_6D_6$ immediately turns colorless upon addition of $C_2H_4$ to an NMR tube at 1 atm or 250 mm pressure. NMR spectroscopy shows complete conversion to $OsHCl(\eta^2\text{-}H_2C{=}CH_2)(CO)(P^iPr_3)_2$. $^1H$ NMR

(+20 °C, $C_6D_6$): $\delta$ −4.59 (br t, $J_{HP}$ = 26.1 Hz, OsH), 1.20 (overlapping m, PCHC$H_3$), 2.68 (m, PCH), 2.94 (br, $v_{1/2}$ = 17.5 Hz, $\eta^2$-$H_2C$=$CH_2$), 5.26 (br, free $C_2H_4$); $^{31}P\{^1H\}$ NMR (+20 °C, $C_6D_6$): $\delta$ 13.1. Sharpening of the signals for the hydride and free $C_2H_4$ is observed in the $^1H$ NMR spectrum upon cooling to −20 °C. No evidence for any other products is seen after mixing for 5 h at +25 °C.

**Reaction of OsDCl(CO)($P^iPr_3$)$_2$ with $C_2H_4$.** An orange solution of OsDCl(CO)($P^iPr_3$)$_2$ in $C_6H_6$ immediately turns colorless upon addition of $C_2H_4$ in the reaction NMR tube at 250 mm pressure. After mixing at +25 °C for 5 h, $^1H$, $^2H$ and $^{31}P$ NMR show complete conversion to the $\eta^2$-ethylene adduct. $^1H$ NMR (+20 °C, $C_6H_6$): $\delta$ 1.21 (overlapping m, PCHC$H_3$), 2.68 (m, PCH), 2.92 [br, $\eta^2$-$C_2H$(D)$_4$], 5.26 [br, free $C_2H$(D)$_4$]; $^2H\{^1H\}$ NMR (+20 °C, $C_6H_6$): $\delta$ −4.58 (br, Os–D), 2.92 [$\eta^2$-$C_2H$(D)$_4$]; $^{31}P\{^1H\}$ NMR (+20 °C, $C_6H_6$): $\delta$ 13.1. After heating at +65 °C for 23 h, $^1H$ NMR shows the growth of a broad OsH signal of the $\eta^2$-ethylene adduct at −4.61 ppm, and a decrease in intensity of peaks at 2.92 ppm (coordinated ethylene) and at 5.26 ppm (free ethylene). $^2H\{^1H\}$ NMR shows a decrease in intensity for the OsD signal at −4.58 ppm and an increase in intensity of the signal for coordinated deuterated ethylene at 2.92 ppm.

**Variable-temperature NMR study of OsHCl($\eta^2$-$H_2C$=$CH_2$)(CO)($P^iPr_3$)$_2$.** A colorless solution of OsHCl(CO)($P^iPr_3$)$_2$ in $C_6D_6$ under 1 atm $C_2H_4$ pressure shows complete conversion to OsHCl($\eta^2$-$H_2C$=$CH_2$)(CO)($P^iPr_3$)$_2$. Upon increasing the temperature from +20 to +70 °C, $^1H$ NMR shows progressive broadening of the signals for free (5.26 ppm) and coordinated (2.92 ppm) ethylene and for the hydride (−4.58 ppm). At +20 °C, $v_{1/2}$(free $C_2H_4$) = 12.8 Hz, $v_{1/2}$($\eta^2$-$C_2H_4$) = 17 Hz, and the OsH peak is a well-defined triplet. At +70 °C, $v_{1/2}$(free $C_2H_4$) = 364 Hz, the signal for $\eta^2$-$C_2H_4$ is so broad that it cannot be seen, and the OsH signal is a broad peak at −5.3 ppm. Upon a temperature increase from +20 to +70 °C, $^{31}P\{^1H\}$ NMR shows a significant broadening and shifting of the signal for OsHCl($\eta^2$-$H_2C$=$CH_2$)(CO)($P^iPr_3$)$_2$ from 13.1 (+20 °C) to 14.6 ppm (+70 °C). No evidence for any other products is seen at any temperature.

**Reaction of OsHCl(CO)($P^iPr_3$)$_2$ with $C_2D_4$.** An orange solution of OsHCl(CO)($P^iPr_3$)$_2$ in $C_6H_6$ immediately turns colorless upon addition of $C_2D_4$ in the reaction NMR tube at 500 mm pressure. After mixing at +60 °C for 27 h, $^1H$, $^2H$ and $^{31}P$ NMR show complete conversion to the $\eta^2$-ethylene adduct. $^1H$ NMR at +20 °C shows the presence of traces of OsH (t, −4.58 ppm), $\eta^2$-$C_2H$(D)$_4$ (2.92 ppm) and free $C_2H$(D)$_4$ (5.26 ppm). $^2H\{^1H\}$ NMR of this sample shows an OsD signal (−4.58 ppm) and two major signals of $\eta^2$-$C_2H$(D)$_4$ (2.92 ppm) and dissolved $C_2H$(D)$_4$ (5.26 ppm).

**Reaction of RuHCl(CO)($P^iPr_3$)$_2$ with $C_2D_4$.** An orange solution of RuHCl(CO)($P^iPr_3$)$_2$ in $C_6H_6$ does not change color upon addition of $C_2D_4$ in the reaction NMR tube at 1 atm pressure. $^1H$, $^2H$ and $^{31}P$ NMR show the absence of $\eta^2$-ethylene adduct or ethyl complex formation. The $^1H$ NMR taken after 27 h at 60 °C shows an almost complete loss of the RuH signal of RuHCl(CO)($P^iPr_3$)$_2$ at −24.36 ppm, and $^2H\{^1H\}$ NMR shows a strong RuD signal at the same chemical shift.

**Reaction of RuHCl(CO)($P^iPr_2Ar^F$)$_2$ with $C_2H_4$.** A yellow–orange solution of RuHCl(CO)($P^iPr_2Ar^F$)$_2$ in $C_6D_6$ immediately becomes colorless, then rosy in 10 min upon addition of a *ca.* 20-fold excess of $C_2H_4$ to the NMR tube. $^1H$, $^{31}P\{^1H\}$ and $^{19}F\{^1H\}$ NMR at +20 °C indicate the formation of two products: RuHCl(CO)($\eta^2$-$C_2H_4$)($P^iPr_2Ar^F$)$_2$ and Ru($CH_2CH_3$)Cl(CO)($P^iPr_2Ar^F$)$_2$. $^1H$ NMR ($C_6D_6$, +20 °C): $\delta$ −10.93 (br, RuH), 0.83, 1.02 (m, PCHC$H_3$), 2.44, 2.65, 2.98 (m, PCH), 2.77 (br, $\eta^2$-$C_2H_4$), 5.26 (br, free $C_2H_4$), 7.76, 7.78 [*p*-3,5-$(CF_3)_2C_6H_2H$], 8.42, 8.48 [*o*-3,5-$(CF_3)_2C_6H_2H$]; $^{31}P\{^1H\}$ NMR ($C_6D_6$, +20 °C): $\delta$ 40.8 [26%, Ru($CH_2$-$CH_3$)Cl(CO)($P^iPr_2Ar^F$)$_2$], 54.4 [br, 74%, RuHCl(CO)($\eta^2$-$C_2H_4$)($P^iPr_2Ar^F$)$_2$]; $^{19}F\{^1H\}$ NMR ($C_6D_6$, +20 °C): $\delta$ −63.84, [33%, Ru($CH_2CH_3$)Cl(CO)($P^iPr_2Ar^F$)$_2$], −63.77 [67%, RuHCl(CO)($\eta^2$-$C_2H_4$)($P^iPr_2Ar^F$)$_2$]. Upon cooling to +7 °C, the broad RuH signal of RuHCl(CO)($\eta^2$-$C_2H_4$)($P^iPr_2Ar^F$)$_2$ in $^1H$ NMR moves to −8.36 ppm, and the $^{31}P\{^1H\}$ NMR signal for the adduct is sharper and observed at 52.9 ppm. When ethylene is removed from this solution by four freeze–pump–thaw cycles, the only observed product by NMR is RuHCl(CO)($P^iPr_2Ar^F$)$_2$; $^1H$ NMR ($C_6D_6$, +20 °C): $\delta$ −24.86 (t, $J_{HP}$ = 18.8 Hz, RuH); $^{31}P$ NMR: $\delta$ 60.4.

### Computational details

The calculations were carried out using the GAUSSIAN 98[22] set of programs within the framework of DFT at the B3PW91 level.[23,24] LANL2DZ effective core potentials (quasi-relativistic for the metal centers) were used to replace the 28 innermost electrons of Ru,[25] the 60 innermost electrons of Os[25] as well as the 10 core electrons of Cl and P.[26] The associated double-$\zeta$ basis set was used[25,25] and was augmented by a d polarization function for Cl and P.[27] The other atoms were represented by a 6-31 (d,p) basis set (5d). Full geometry optimization was performed with no symmetry restriction and the nature of the minima was assigned by analytical frequency calculations.

## Acknowledgements

This work was supported by the University of Montpellier 2, the CNRS, and the Indiana University computer center. We also thank the donors of the Petroleum Research Fund, administered by the American Chemical Society.

## References and notes

1 A. Andriollo, M. A. Esteruelas, U. Meyer, L. A. Oro, R. A. Sanchez-Delgado, E. Sola, C. Valero and H. Werner, *J. Am. Chem. Soc.*, 1989, **111**, 7431.
2 H. Werner, W. Stüer, J. Wolf, M. Laubender, B. Weberndörfer, R. Herbst-Irmer and C. Lehmann, *Eur. J. Inorg. Chem.*, 1999, 1889.
3 M. A. Esteruelas and H. Werner, *J. Organomet. Chem.*, 1986, **303**, 221.
4 H. Werner, U. Meyer, K. Peters and H. G. von Schnering, *Chem. Ber.*, 1989, **122**, 2097.
5 (*a*) H. Werner, M. A. Esteruelas and H. Otto, *Organometallics*, 1986, **5**, 2295; (*b*) M. A. Esteruelas, F. J. Lahoz, E. Onate, L. A. Oro and B. Zeier, *Organometallics*, 1995, **14**, 4685; (*c*) M. A. Esteruelas, L. A. Oro and C. Valero, *Organometallics*, 1995, **14**, 1596; (*d*) M. A. Esteruelas, A. V. Gomez, F. J. Lahoz, A. M. Lopez, E. Onate and L. A. Oro, *Organometallics*, 1996, **15**, 3423; (*e*) M. A. Esteruelas, F. Liu, E. Onate, E. Sola and B. Zeier, *Organometallics*, 1997, **16**, 2919; (*f*) M. A. Esteruelas, L. A. Oro and C. Valero, *Organometallics*, 1992, **11**, 3362.
6 This was briefly reported,[3] but the resonance assigned to coordinated ethylene is in fact that of free ethylene.
7 There is no evidence of deuteration at any site on the phosphine $^i$Pr groups.
8 A. V. Marchenko, H. Gérard, O. Eisenstein and K. G. Caulton, *New J. Chem.*, 2001, **25**, 1244.
9 J. A. M. Simoes and J. L. Beauchamp, *Chem. Rev.*, 1990, **90**, 629.
10 H. Gérard, E. Clot and O. Eisenstein, *New J. Chem.*, 1999, **23**, 495.
11 H. Werner, W. Stüer, M. Laubender, C. Lehmann and R. Herbst-Irmer, *Organometallics*, 1997, **16**, 2236.
12 D. Huang, G. J. Spivak and K. G. Caulton, *New J. Chem.*, 1998, **22**, 1023.
13 (*a*) G. J. Spivak, J. N. Coalter, M. Oliván, O. Eisenstein and K. G. Caulton, *Organometallics*, 1998, **17**, 999; (*b*) D. Huang, M. Oliván, J. C. Huffman, O. Eisenstein and K. G. Caulton, *Organometallics*, 1998, **17**, 4700.

14 G. Frenking and N. Fröhlich, *Chem. Rev*., 2000, **100**, 717.
15 See, however: A. Nicolaides and W. T. Borden, *J. Am. Chem. Soc*., 1991, **113**, 6750.
16 M. Oliván, E. Clot, O. Eisenstein and K. G. Caulton, *Organometallics*, 1998, **17**, 3091.
17 (*a*) J. Silvestre and R. Hoffmann, *Helv. Chim. Acta*, 1985, **68**, 1461; (*b*) Y. Wakatsuki, N. Koga, H. Yamazaki and K. Morokuma, *J. Am. Chem. Soc*., 1994, **116**, 8105; (*c*) Y. Wakatsuki, N. Koga, H. Werner and K. Morokuma, *J. Am. Chem. Soc*., 1997, **119**, 360; (*d*) R. Stegman and G. Frenking, *Organometallics*, 1998, **17**, 2089; (*e*) C. Garcia-Yebra, C. López-Mardomingo, M. Fajardo, A. Antiñolo, A. Otero, A. Rodriguez, A. Vallat, D. Lucas, Y. Mugnier, J. J. Carbó, A. Lledos and C. Bo, *Organometallics*, 2000, **19**, 1749; (*f*) E. Perez-Carreno, P. Paoli, A. Ienco and C. Mealli, *Eur. J. Inorg. Chem*., 1999, **8**, 1315; (*g*) V. I. Bakhmutov, J. Bertrán, M. A. Esteruelas, A. Lledós, F. Maseras, J. Modrego, L. A. Oro and E. Sola, *Chem. Eur. J*., 1996, **7**, 815.
18 A. V. Marchenko, M. Jimenez-Tenorio, P. Valerga, M. C. Puerta and K. G. Caulton, *Inorg. Chem*., in press.
19 J. U. Notheis, R. H. Heyn and K. G. Caulton, *Inorg. Chim. Acta*, 1995, **229**, 187.
20 C. S. Yi and D. W. Lee, *Organometallics*, 1999, **18**, 5152.
21 W. J. Hehre, L. Radom, v. R. Schleyer and J. A. Pople, *Ab Initio Molecular Orbital Theory*, Wiley, New York, 1986, p. 282.
22 M. J. Frisch, G. W. Trucks, H. B. Schlegel, G. E. Scuseria, M. A. Robb, J. R. Cheeseman, V. G. Zakrzewski, J. A. Montgomery, Jr., R. E. Stratmann, J. C. Burant, S. Dapprich, J. M. Millam, A. D. Daniels, K. N. Kudin, M. C. Strain, O. Farkas, J. Tomasi, V. Barone, M. Cossi, R. Cammi, B. Mennucci, C. Pomelli, C. Adamo, S. Clifford, J. Ochterski, G. A. Petersson, P. Y. Ayala, Q. Cui, K. Morokuma, D. K. Malick, A. D. Rabuck, K. Raghavachari, J. B. Foresman, J. Cioslowski, J. V. Ortiz, A. G. Baboul, B. B. Stefanov, G. Liu, A. Liashenko, P. Piskorz, I. Komaromi, R. Gomperts, R. L. Martin, D. J. Fox, T. Keith, M. A. Al-Laham, C. Y. Peng, A. Nanayakkara, C. Gonzalez, M. Challacombe, P. M. W. Gill, B. Johnson, W. Chen, M. W. Wong, J. L. Andres, C. Gonzalez, M. Head-Gordon, E. S. Replogle and J. A. Pople, GAUSSIAN 98, Rev. A7, Gaussian Inc., Pittsburgh, PA, 1998.
23 A. D. Becke, *J. Chem. Phys*., 1993, **98**, 5648.
24 J. P. Perdew and Y. Wang, *Phys. Rev. B*, 1992, **45**, 13244.
25 P. G. Hay and W. R. Wadt, *J. Chem. Phys*., 1985, **82**, 299.
26 W. R. Wadt and P. J. Hay, *J. Chem. Phys*., 1985, **82**, 284.
27 A. H. Höllwarth, M. B. Böhme, S. Dapprich, A. W. Ehlers, A. Gobbi, V. Jonas, K. F. Köhler, R. Stegmann, A. Veldkamp and G. Frenking, *Chem. Phys. Lett*., 1993, **208**, 237.
28 (*a*) P. C. Hariharan and J. A. Pople, *Theor. Chim. Acta*, 1973, **28**, 213; (*b*) W. J. Hehre, R. Ditchfield and J. A. Pople, *J. Chem. Phys*., 1972, **56**, 2257.